

LA-4740-MS

AN INFORMAL REPORT

E.1

The Reduction of Mesh Tangling
in Two-Dimensional Lagrangian Hydrodynamics Codes
by the Use of Viscosity, Artificial Viscosity, and TTS
(Temporary Triangular Subzoning for Long, Thin Zones)



For Reference

Not to be taken from this room



Los Alamos
scientific laboratory
of the University of California
LOS ALAMOS, NEW MEXICO 87544

This report was prepared as an account of work sponsored by the United States Government. Neither the United States nor the United States Atomic Energy Commission, nor any of their employees, nor any of their contractors, subcontractors, or their employees, makes any warranty, express or implied, or assumes any legal liability or responsibility for the accuracy, completeness or usefulness of any information, apparatus, product or process disclosed, or represents that its use would not infringe privately owned rights.

This report, like other special-purpose documents in the LA. . .MS series, has not been reviewed or verified for accuracy in the interest of prompt distribution.

Printed in the United States of America. Available from
National Technical Information Service
U. S. Department of Commerce
5285 Port Royal Road
Springfield, Virginia 22151
Price: Printed Copy \$3.00; Microfiche \$0.95

LA-4740-MS
An Informal Report
UC-32

ISSUED: November 1971



The Reduction of Mesh Tangling
in Two-Dimensional Lagrangian Hydrodynamics Codes
by the Use of Viscosity, Artificial Viscosity, and TTS
(Temporary Triangular Subzoning for Long, Thin Zones)

by

Philip L. Browne
Karl B. Wallick



THE REDUCTION OF MESH TANGLING IN TWO-DIMENSIONAL LAGRANGIAN HYDRODYNAMICS CODES BY THE
USE OF VISCOSITY, ARTIFICIAL VISCOSITY, AND TTS (TEMPORARY TRIANGULAR SUBZONING FOR LONG,
THIN ZONES).

by

Philip L. Browne and Karl B. Wallick

ABSTRACT

Several related studies of compressible, two-dimensional Lagrangian hydrodynamics are described. Reduction of mesh tangling, particularly in problems that have long thin zones is emphasized. The topics discussed are: a general method of deriving the momentum equation in difference form, incorporation of the viscosity-stress tensor into this method, use of the viscous-stress tensors to add a two-dimensional form of the Richtmyer von-Neumann artificial viscosity, and a device called "temporary triangular subzoning" (TTS) to delay the transmittal of artificial signals that lead to oscillations and tangling in long, thin zones. The last two methods have not been tested thoroughly, but have certainly eliminated a great deal of the twisting and tangling in several test problems. These methods also retain spherical, cylindrical, and plane symmetry in problems of that type. The last proposal, the TTS, may introduce some stiffness into the mesh, but we hope that with further experimentation this can be reduced. Our basic purpose is not to propose these concepts as polished cure-alls for mesh tangling, but to present the basic ideas which, to us, seem sound and worth consideration.

INTRODUCTION

During the past 10 years, we have devoted considerable time to the study of numerical calculations in two-dimensional (r,z) Lagrangian hydrodynamics for compressible flow. Lagrangian calculations have many advantages, but in two dimensions one great disadvantage is the tendency for the mesh to become tangled. In many cases this is caused by the real, physical motion of the fluid, but we have noticed many situations in which we believe this twisting to be nonphysical. Small perturbations of one kind or another become magnified in both time and space. This seems to be especially true when long, thin zones (large aspect ratios) are present in the mesh. The ideal solution would be to avoid meshes that have large aspect ratios, but sometimes other physical requirements of the problem or the related calculations prevent this. For this report,

we assume that long thin zones are sometimes necessary, and attempt to suggest methods for getting along with them.

This report consists of four parts, all related and necessary to each other. It would be preferable to issue each part as a separate report, giving more detail, and we may try to do so in the future. However, as a temporary expediency to present the basic ideas, we include all these related topics here, and consequently present many results and concepts without proof or detailed explanations. Because some of the calculations in which these methods have been used involve items unrelated to the problem of tangled meshes, no results or examples are given in detail. All numerical work was done with a code named JANUS, parts of which have been described elsewhere.^{1,2}

The first section of the report describes the model and method used to difference the equation of

conservation of momentum. This method, called Integrated Gradients, was developed about eight years ago.³ The basic idea is to derive the difference equations by using surface integrals of the pressure to calculate the momentum transfer, rather than to difference the differential equation. Others have used similar arguments in other codes.^{4,5} We feel that these integral methods are generally superior to differencing the differential equation directly, as they go back to the basic physical ideas used in deriving the differential equation, and this approach often clarifies the assumptions that must be made (for example in boundary cases).

The second section describes a way to add the viscous-stress tensor to the hydrodynamic calculations.⁶ This, again, is done with surface integrals, and for the same reasons. The viscosity calculations were added primarily in the hope of using them to damp out oscillations in the mesh. This worked quite well in many problems. The viscosity coefficients required were larger than those that would arise owing to any physical effects, and they appeared to depend on such things as density and mesh spacing. However, with some experimenting, we could often use this method to run problems that would have become very tangled otherwise. In other words, it was used as a velocity smoothing agent rather than a real viscosity effect. Of course, the way in which it was set up would enable it to be used directly for real viscosity calculations.

The third section describes a method for setting up a two-dimensional artificial viscosity.⁷ This method was based on the model chosen for the viscosity calculation described in the previous paragraph, and, indeed, the artificial viscosity was incorporated into the viscous stress tensor. We found that this type of artificial viscosity was very necessary, particularly in problems with large aspect ratios.

The last section introduces a concept that also seems to be needed in problems with large aspect ratios. This is the necessity to isolate the two ends of long, thin zones temporarily in order to delay or prevent an unphysical, numerical effect from being transmitted from one end of the zone to the other end in one cycle. The method we devised amounts to treating a zone as if it has triangular subzones temporarily, and then allowing the energy

to be smeared over the whole zone. This, again, was an outgrowth of the model derived for the viscosity calculations.

The last two concepts were developed only within the last year, and have not been thoroughly tested. However, they seem to prevent mesh tangling in some very difficult situations. Moreover, they make sense, at least to the authors, who have felt the need for something like this for several years. We have done little or no work on such things as the stability conditions required to go along with these calculations. We have done quite a bit of work to ensure that some simple problems (planes, cylinders, and spheres) retain their symmetry.

I. INTEGRATED GRADIENTS

A. The Integral Form of the Momentum Equation

Using integrals, one can write the equation of momentum conservation for a blob of fluid contained in a volume, V , in the Lagrangian form

$$\int_V \rho \frac{d\vec{v}}{dt} dV = - \int_S P d\vec{S} . \quad (I-1)$$

If we assume that all the material in V has the same acceleration, $d\vec{v}/dt$, (i.e., use the mean-value theorem), then because $\int \rho dV$ gives the mass, M , enclosed by S , we can write

$$M \frac{d\vec{v}}{dt} = - \int_S P d\vec{S} . \quad (I-2)$$

B. Zone Quantities and Point Quantities

Consider a section of typical Lagrangian mesh (Fig. 1) in an (r,z) coordinate system. Usually each zone $(i+\frac{1}{2}, j+\frac{1}{2})$ has associated with it such things as mass, pressure, density or specific volume, temperature, artificial viscosity, and specific internal energy, which we denote by

$$(M, P, \rho, \tau, T, q, E)_{i+\frac{1}{2}, j+\frac{1}{2}} . \quad (I-3)$$

All of these are the quantities needed or evaluated by the equation of conservation of internal energy, which we write as

$$\frac{dE}{dt} = -(P+q) \frac{d\tau}{dt} . \quad (I-4)$$

Usually each point (or vertex) has associated with it such things as coordinates, velocities, and accelerations, which we denote by

$$(r, z, \dot{r}, \dot{z}, \ddot{r}, \ddot{z})_{i,j}.$$

All of these are the quantities needed or evaluated by the equation of motion, Eq. (I-2). However, we note that Eq. (I-2), for complete definition requires a mass, M , to be associated with the point, and a surface, S , enclosing that mass. Many codes define the masses used in some arbitrary manner, but we attempt to be more esthetic about it, enabling us to better visualize what we are doing.

$$\int_{\ell}^{\ell+1} d\vec{S} = \int_{\ell}^{\ell+1} d\vec{S}' + \oint_{\phi} d\vec{S} \text{ is independent of}$$

the path S' from ℓ , $\ell+1$, (I-5)

and, in more detail,

$$\int_{\ell}^{\ell+1} d\vec{S} = \vec{i} \frac{\phi}{2} \left[-z_{\ell} r_{\ell} - r(z_{\ell} - z_{\ell+1}) - z(r_{\ell+1} - r_{\ell}) + z_{\ell+1} r_{\ell+1} \right] + \vec{k} \frac{\phi}{2} (r_{\ell}^2 - r_{\ell+1}^2), \quad (I-6)$$

where \vec{i} and \vec{k} are unit vectors in the r and z di-

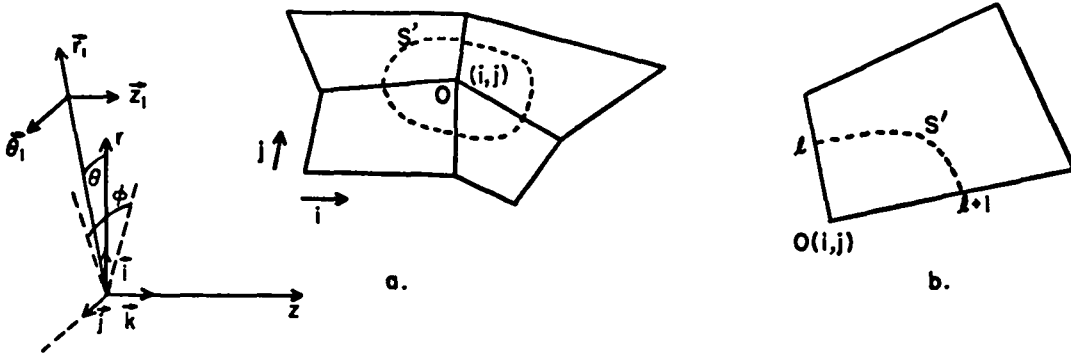


Fig. 1. A sample point and a sample zone in a Lagrangian mesh.

C. Evaluation of $\int Pd\vec{S}$.

Recall that this is a figure of revolution about the z axis, and that each zone represents an element of volume in which the scalar quantities are constant. Vector quantities will be constant in magnitude but will vary direction with θ . For our purposes we cannot consider a revolution of 2π about the axis, for then the integrals of all forces in the r direction will vanish. Hence, we consider a revolution of small angle, ϕ , about the z axis. This means that the volume considered is wedge-shaped, and the forces on the sides of the wedge must be considered.

Suppose we are working with point (i,j) and consider any surface S' in zone $(i+\frac{1}{2}, j+\frac{1}{2})$, Fig. 1a, enclosing the part of the mass from that zone to be associated with (i,j) in the momentum equation. One can prove (proof omitted due to length) that if one adds the forces caused by integration of the pressure over the front and rear faces of the wedge to the forces caused by integrating P over S' , the result is independent of the path from ℓ to $\ell+1$. We indicate this by the notation

rections at $\theta = 0$.

For this particular mass there are also forces along the surfaces formed by lines $(0,\ell)$ and $(0,\ell+1)$. If we denote the pressures along these sides by $P_{\ell}^{\ell+\frac{1}{2}}$, $P_{\ell+1}^{\ell+\frac{1}{2}}$, then the total force on the mass being considered in Fig. 1b is given by

$$\vec{F}_{\ell+\frac{1}{2}} = (-\int Pd\vec{S})_{\ell+\frac{1}{2}} = - \left(P_{\ell}^{\ell+\frac{1}{2}} \int_{\ell}^{\ell+\frac{1}{2}} d\vec{S} + P_{\ell+1}^{\ell+\frac{1}{2}} \int_{\ell+1}^{\ell+\frac{1}{2}} d\vec{S} \right) - P_{\ell+\frac{1}{2}} \left(\int_{\ell}^{\ell+1} d\vec{S}' + \oint_{\phi} d\vec{S} \right)$$

$$\left\{ \begin{aligned} \vec{F}_{\ell+\frac{1}{2}} &= \vec{i} \frac{\phi}{2} \left[(P_{\ell}^{\ell+\frac{1}{2}} - P_{\ell+1}^{\ell+\frac{1}{2}}) (z - z_{\ell}) (r + r_{\ell}) + (P_{\ell+1}^{\ell+\frac{1}{2}} - P_{\ell}^{\ell+\frac{1}{2}}) \right. \\ &\quad \times (z_{\ell+1} - z) (r_{\ell+1} + r) \\ &\quad + \vec{k} \frac{\phi}{2} \left[(P_{\ell}^{\ell+\frac{1}{2}} - P_{\ell+1}^{\ell+\frac{1}{2}}) (r_{\ell} - r) (r + r_{\ell}) + (P_{\ell+1}^{\ell+\frac{1}{2}} - P_{\ell}^{\ell+\frac{1}{2}}) \right. \\ &\quad \times (r - r_{\ell+1}) (r + r_{\ell+1}) \left. \right] \end{aligned} \right. \quad (I-7)$$

This is the general force acting on the mass in zone $(i+\frac{1}{2}, j+\frac{1}{2}) = \ell+\frac{1}{2}$ defined by any path S' joining ℓ to $\ell+1$.

It might be well to add a word about conserva-

tion of momentum. Because $\int P d\vec{S}$ is a momentum flux term, if one desires to conserve momentum exchange between two adjacent masses when using this method, he must require that

$$\int_0^k P_{\ell}^{\ell+\frac{1}{2}} d\vec{S} = -\int_{\ell}^0 P_{\ell}^{\ell-\frac{1}{2}} d\vec{S}.$$

Because we assume the P's to be constant along $(0, \ell)$,

$$P_{\ell}^{\ell+\frac{1}{2}} = P_{\ell}^{\ell-\frac{1}{2}} = P_{\ell}. \quad (I-8)$$

We have found that a good definition of P_{ℓ} is given by

$$P_{\ell} = \frac{1}{2}(P_{\ell-\frac{1}{2}} + P_{\ell+\frac{1}{2}}). \quad (I-8a)$$

D. Defining the Masses for the Momentum Equation

As previously mentioned, once the positions of ℓ and $\ell+1$ have been selected along the lines joining 0 to the adjacent points, the value of $\vec{F}_{\ell+\frac{1}{2}}$ is independent of the path S' chosen in the zone. The path S' can be considered as defining the mass from zone $\ell+\frac{1}{2}$ to be associated with 0 for the momentum equation. There are many ways in which S' could be chosen for the set of zones about point 0. One condition that comes to mind is to choose S' (Fig. 1a) so that 0 is at the center of mass of the material enclosed by S' . But even this could be done in many ways.

After much thought, analytic work and numerical experimentation, the best method we found was the MAC-0 (midpoint, average-centroid at time zero) method. In this method, at the start of a problem, the points ℓ are chosen as the midpoints of the sides, and these are joined by straight lines to a point, 8, that is the average of the four corners (Fig. 2). This gives four subzone masses in each zone. There are thus four masses around point 0 which are associated with it for momentum calculations.

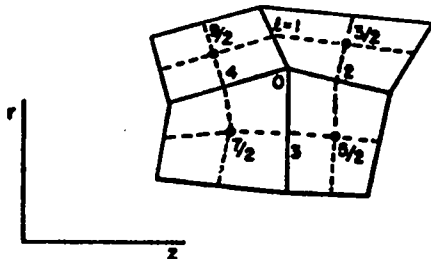


Fig. 2. Definition of the MAC-0 masses.

Although the MAC-0 method of defining masses does require more storage than some other methods (such as using a given fraction, like $\frac{1}{4}$, of the mass of each zone), it has a number of advantages. First, conceptually, the masses used with one point, 0, do not overlap the masses used with adjacent points. Second, when one performs the momentum transfer by calculating $\int P d\vec{S}$, momentum is conserved; i.e., momentum taken from 0 is transferred to the adjacent points because the integrations can be visualized as being performed in opposite directions along a common side. This idea of conserving quantities, usually fluxes, is very important in physics, and it seems that it should be used, if possible, in numerical computations.⁸ Third, in a series of test runs on some simple plane problems with a small initial distortion of the mesh, the MAC-0 method enabled the problems to run about twice as far before the distortions become severe.⁹ Fourth, this model enabled us to develop the method of rezoning² which conserved mass, momentum, and total energy of the model exactly.

E. Combining Forces and Masses to Obtain Accelerations.

To calculate the acceleration of point 0, all that remains is to decide how to combine the masses and forces from the various subzones about 0 to represent Eq. (I-2).

1. IOT (Integral Gradient Total). The most straightforward method, represented pictorially in Fig. 3a, is to integrate around the four subzone masses associated with the point 0, which gives

$$\frac{d\vec{v}}{dt} = \left(\sum_{\ell=1}^4 \vec{F}_{\ell+\frac{1}{2}} \right) / \left(\sum_{\ell=1}^4 M_{\ell+\frac{1}{2}} \right). \quad (I-9)$$

Unfortunately, in spherical problems with equal angular spacing, this method does not give uniform spherical motion, a very desirable feature to have. This has been verified analytically as well as numerically. The method works well in planes and cylinders with uniform spacing. Using Eq. (I-7), the general formula for $\sum_{\ell} \vec{F}_{\ell+\frac{1}{2}}$ works out quite simply, owing to cancellation of terms, as

$$\begin{aligned} \sum_{\ell=1}^4 \vec{F}_{\ell+\frac{1}{2}} &= \bar{i} \frac{g}{2} \sum_{\ell=1}^4 \left[(P_{\ell-\frac{1}{2}} - P_{\ell+\frac{1}{2}})(z-z_{\ell})(r+r_{\ell}) \right] \\ &+ \bar{k} \frac{g}{2} \sum_{\ell=1}^4 \left[(P_{\ell-\frac{1}{2}} - P_{\ell+\frac{1}{2}})(r_{\ell}-r)(r+r_{\ell}) \right]. \end{aligned} \quad (I-10)$$

2. IGA (Integral Gradient-Average). A less straightforward method is to calculate an acceleration for each subzone, Fig. 3b, and then average these accelerations. This gives

$$\frac{d\vec{v}}{dt} = \frac{1}{4} \sum_{\ell=1}^4 \left(\frac{\vec{F}_{\ell+\frac{1}{2}}}{M_{\ell+\frac{1}{2}}} \right), \quad (I-11)$$

which cannot be simplified much by substituting from Eq. (I-7). [Note that a mass-weighted average, which seems more logical from many points of view, gives IGT, Eq. (I-9).] Unlike IGT, IGA can be shown, numerically and analytically, to give spherical motion in a spherical problem with uniform angular spacing. It gives exactly the same results as IGT in cylindrical and plane problems. After several years of working with both IGT, and IGA we tend to prefer the latter.

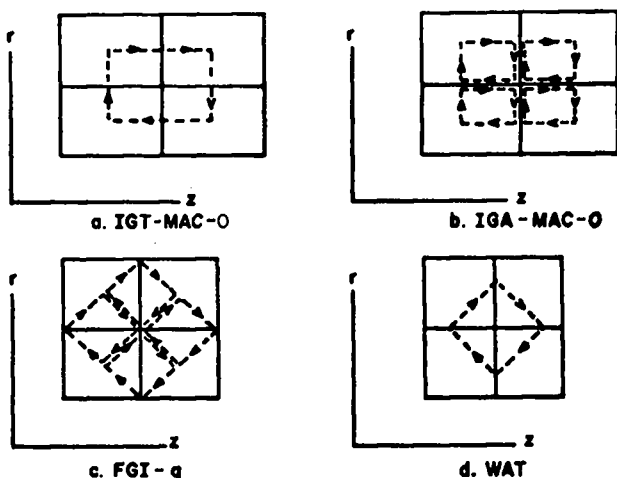


Fig. 3. Representations of various gradients (dashed lines show paths of integration for each element of mass).

3. FGI-q (Force Gradient I-q Mass). We could obtain the acceleration used in MAGEE,¹⁰ from Eq. (I-7), by an averaging and integration method illustrated in Fig. 3c. The general form is

$$\frac{d\vec{v}}{dt} = \frac{1}{4} \sum_{\ell=1}^4 \left(\frac{\vec{F}_{\ell-\frac{1}{2}} + \vec{F}_{\ell+\frac{1}{2}}}{M_{\ell-\frac{1}{2}} + M_{\ell+\frac{1}{2}}} \right). \quad (I-12)$$

where the M's are one quarter of the zone masses. This type of acceleration calculation also gives spherical motion in a spherical problem with uniform angular spacing.

4. WAT. The acceleration calculation used in WAT¹¹

can be obtained, using Eq. (I-7), by integrating around a diamond-shaped surface (Fig. 3d), where the points on the sides lie 2/3 of the way out to the next vertex. We have done no numerical or analytic work with this method on spherical or other special problems.

F. Boundary Cases.

Setting up proper boundary calculations is often more difficult than the general case. However, study of the boundaries often leads to clues as to how the general case should be handled. Our general criterion for boundary cases has been that in plane, cylindrical, and spherical problems they should give the same acceleration as the general case (i.e., corresponding interior points).

For sliding boundaries (Fig. 4), whether at constant r, constant z, or at some angle to the axes, the general procedure is the same. (We are considering only IGA-MACO). In Eq. (I-7), let

$$\begin{aligned} P_{\ell-1}^{\ell-\frac{1}{2}} &= P_{\ell-\frac{1}{2}} \quad \text{for zone } \ell-\frac{1}{2}, \\ P_{\ell+1}^{\ell+\frac{1}{2}} &= P_{\ell+\frac{1}{2}} \quad \text{for zone } \ell+\frac{1}{2}. \end{aligned} \quad (I-13a)$$

Then, in Eq. (I-11),

$$\frac{d\vec{v}}{dt} = \frac{1}{2} \left(\frac{\vec{F}_{\ell-\frac{1}{2}}}{M_{\ell-\frac{1}{2}}} + \frac{\vec{F}_{\ell+\frac{1}{2}}}{M_{\ell+\frac{1}{2}}} \right). \quad (I-13b)$$

The final operation is to keep only the component of the acceleration tangent to the surface defined by the boundary. (I-13c)

This is equivalent to the often used method of reflecting the two zones across the boundary and using the general case. For a slanting boundary, this requires considerable care.

For a free surface the procedure is the same, except that along the free surface we assume that

$$P_{\ell-1} = P_{\ell+1} = 0. \quad (I-14a)$$

Then use Eq. (I-13b), but not (I-13c). All these methods approach the proper limits, as the spacing is made smaller.

For other types of special points, such as corner points in a mesh, the situation dictates the necessary assumptions. Proper combinations of assump-

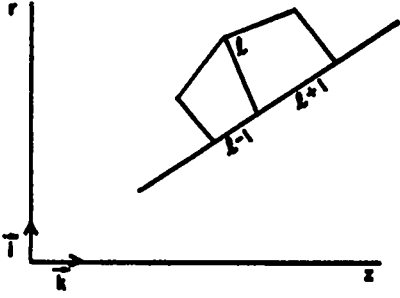


Fig. 4. A sliding boundary or free surface.

tions for a sliding boundary and a free surface have worked properly as far as we can tell.

G. Conclusion.

All the statements made in this section have been verified either by analytic analysis or by numerical calculations with the JANUS code. We definitely prefer the MAC-0 method of defining the masses associated with points. We prefer the IGA model of deriving accelerations, mainly because it gives spherical symmetry in a spherical problem with equal angular zoning, whereas IGT does not. The IGT method does seem to slow the growth of distortions slightly, more so than does IGA. However, in any problem in which the mesh already has some distortions, we are convinced that some additional devices, such as those to be described in the next sections, are needed.

II. VISCOSITY

A. The Viscous-Stress Tensor.

To include a viscosity calculation, one must add extra terms to the equations of conservation of momentum and energy. After looking into this at considerable length, we decided to use the integral form of the equation of motion, as we did for the pressure gradient. This is somewhat more complicated, because the true incorporation of viscosity requires a tensor, called the viscous-stress tensor.

We represent the viscous-stress tensor^{12,13} by

$$\sigma_{ij} = \mu \left(\frac{\partial v_i}{\partial x_j} + \frac{\partial v_j}{\partial x_i} \right) + \delta_{ij} \lambda (\nabla \cdot \vec{v}) . \quad (\text{II-1})$$

In any coordinate system, σ_{ij} represents the flux of i momentum transferred across an area perpendicular to the j direction owing to viscous forces (i.e., with no corresponding mass transfer).

In an r, z coordinate system (Ref. 12, p. 181),

the nine-component tensor is

$$\begin{aligned} \sigma_{rr} &= \mu(2\dot{r}_r) + \lambda(\nabla \cdot \vec{v}) & \sigma_{r\theta} &= 0 & \sigma_{rz} &= \mu(\dot{r}_z + \dot{z}_r) \\ \sigma_{i j} &= \sigma_{\theta r} = 0 & \sigma_{\theta\theta} &= \mu(2\dot{\theta}) + \lambda(\nabla \cdot \vec{v}) & \sigma_{\theta z} &= 0 \\ \sigma_{zr} &= \mu(\dot{r}_z + \dot{z}_r) & \sigma_{z\theta} &= 0 & \sigma_{zz} &= \mu(2\dot{z}_z) + \lambda(\nabla \cdot \vec{v}) \end{aligned} \quad (\text{II-2})$$

where $\nabla \cdot \vec{v} = \dot{r}_r + \dot{\theta}/r + \dot{z}_z$.

B. The Momentum Equations.

Let us write the momentum equation in terms of a volume of fluid, V .

$$\int_V \rho \frac{dv_i}{dt} \vec{e}_i dV = - \int_V (\nabla p)_i \vec{e}_i dV + \int_V \frac{\partial \sigma_{ik}}{\partial x_k} \vec{e}_i dV , \quad (\text{II-3})$$

where \vec{e}_i are the unit vectors, \vec{r}_1 , $\vec{\theta}_1$, and \vec{z}_1 , as shown in Fig. 1. Repeated subscripts indicate a summation. Using the same arguments proposed in Sec. I, and in Aris,¹² p. 179, we can write this in terms of surface integrals

$$M \frac{d\vec{v}}{dt} = - \int_S p d\vec{S} + \int_S \vec{e}_i \sigma_{ij} dS_j . \quad (\text{II-4})$$

Evaluation of $-\int_S p d\vec{S}$ has been discussed in Sec. I. For the viscous terms, as one integrates over the surface, the \vec{e}_i changes direction, and this must be allowed for. If we substitute for the \vec{e}_i (see Fig. 1) in terms of \vec{i} , \vec{j} , and \vec{k} ,

$$\vec{e}_i = \iota_{in} \vec{i}_n ,$$

or

$$\vec{r}_1 = (\cos \theta) \vec{i} + (\sin \theta) \vec{j} + (0) \vec{k} ,$$

$$\vec{\theta}_1 = (-\sin \theta) \vec{i} + (\cos \theta) \vec{j} + (0) \vec{k} ,$$

$$\vec{z}_1 = (0) \vec{i} + (0) \vec{j} + \vec{k} , \quad (\text{II-5})$$

we have unit vectors that do not change direction with the position of the element on the surface. These can be removed from the integral. Thus, substituting Eq. (II-5) in Eq. (II-4), we have

$$M \frac{d\vec{v}}{dt} = - \int_S p d\vec{S} + \vec{i}_n \int \iota_{in} \sigma_{ik} dS_k . \quad (\text{II-4s})$$

C. Evaluation of Surface Integrals.

Carrying through all the manipulations for the surfaces of a volume formed by rotating a triangle OAB (Fig. 5) through a small angle φ about the z axis, we get a contribution for the last term in Eq. (II-4a).

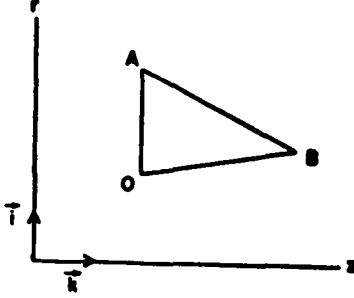


Fig. 5.

$$\begin{aligned} \vec{i}_n \int_{\Delta} \ell_{in} \sigma_{ik} dS_k &= \vec{i}\varphi \left(\int_A^B \sigma_{rr} r dz - \int_A^B \sigma_{rz} r dr \right) \\ &+ \vec{k}\varphi \left(\int_A^B \sigma_{zr} r dz - \int_A^B \sigma_{zz} r dr \right) \\ &- \vec{i}\varphi \int_{\Delta} \sigma_{\theta\theta} r dr dz, \end{aligned} \quad (II-6)$$

where \int_{Δ} indicates integration over the surface formed by rotating AB, and \int_A^B denotes integration over the triangular faces of the wedge formed by the rotation. The integrals over the surfaces formed by rotating OA and OB have not been included, but would be written in the same form as the \int_{Δ} if needed.

If the σ_{ik} are constant over the range of integration, Eq. (II-6) becomes exactly

$$\begin{aligned} \vec{i}\varphi \left[\sigma_{rr} (z_B - z_A) \left(\frac{r_B + r_A}{2} \right) - \sigma_{rz} (r_B - r_A) \left(\frac{r_B + r_A}{2} \right) \right] \\ + \vec{k}\varphi \left[\sigma_{zr} (z_B - z_A) \left(\frac{r_B + r_A}{2} \right) - \sigma_{zz} (r_B - r_A) \left(\frac{r_B + r_A}{2} \right) \right] \\ - \vec{i}\varphi \frac{1}{2} \left[(z_B - z_0)(r_A - r_0) - (z_A - z_0)(r_B - r_0) \right]. \end{aligned} \quad (II-6a)$$

This expression cannot, of course, be substituted directly into Eq. (II-4a), because it applies only to a triangle, whereas for the momentum equation it is necessary to perform the surface integration over all the material considered to be associated with the point. Several decisions must be made. One is how to evaluate the σ 's, and another is what kind of model to use for the complete surface integration of all the masses associated with the point in question. These two decisions are related.

After considerable thought and experimentation, and drawing from previous experience in developing the pressure integrals, we settled on the following methods.

D. Calculating the σ 's.

Evaluation of the σ 's, see Eq. (II-2), requires evaluation of velocity derivatives, \dot{r}_r , \dot{r}_z , \dot{z}_r , and \dot{z}_z . The most straightforward approach is to use triangles. Specifically, if \dot{r} is known at three points, 0, ℓ , and $\ell+1$, assume that \dot{r} is defined by a plane passing through the three known values \dot{r}_0 , \dot{r}_ℓ , and $\dot{r}_{\ell+1}$. Then the derivatives are constant over that triangle, and we can write

$$\begin{aligned} \dot{r}_\ell &= \dot{r}_0 + \dot{r}_r (r_\ell - r_0) + \dot{r}_z (z_\ell - z_0), \\ \dot{r}_{\ell+1} &= \dot{r}_0 + \dot{r}_r (r_{\ell+1} - r_0) + \dot{r}_z (z_{\ell+1} - z_0). \end{aligned} \quad (II-7)$$

These two equations can then be solved for the two unknowns \dot{r}_r and \dot{r}_z . Similar equations hold for \dot{z}_r and \dot{z}_z . The value of \dot{r}/r is obtained by

$$\frac{\dot{r}}{r} = \frac{\dot{r}_0 + \dot{r}_\ell + \dot{r}_{\ell+1}}{r_0 + r_\ell + r_{\ell+1}}. \quad (II-8)$$

E. The Viscous Triangles.

In view of our experience with $\int Pd\vec{S}$ (Sec. I), it occurred to us that we could set up the corresponding viscous calculation in the following manner. Consider a set of zones about a point (Fig. 6).

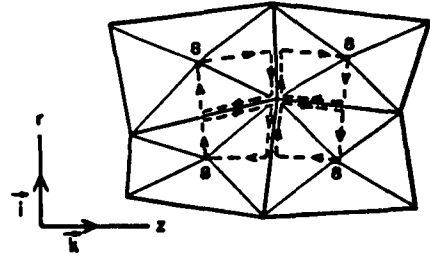


Fig. 6. The viscous triangles.

For each zone, we define² a point, θ , that has as coordinates and velocities the average of those for the four corners of the zone. These points, when connected to the four corners, define four "viscous triangles" in each zone. As described in the previous paragraph, the σ 's can then be evaluated for each of these triangles.

Using the viscous triangles, it is now possible

to propose a method for calculating the viscous terms in the momentum equations by properly defining the surfaces over which the integrations are to be performed. Referring to Fig. 3, we can choose, preferably, either an IGT-MACO or an IGA-MACO method. We have tried both. The IGT-MACO method is simpler, but does not give spherical symmetry in a spherical problem with equal angular spacing (the same as our experience with the pressure integral). The IGA-MACO method is longer, but seems to give proper spherical motion (as was true for the pressure integral). It is represented by the dashed lines in Fig. 6. This method has not been verified analytically, as it was for the pressure integrals.

Note that because the viscous-stress tensor represents a momentum transfer, this scheme gives conservation of momentum between adjacent points in the mesh, as was discussed for the pressure integrals in Sec. I. We feel that this is desirable. Where σ 's are required along a boundary between two viscous triangles, as in IGA-MACO, we use the average of the σ 's on both sides, similar to the pressure argument in Eq. (I-8). Along boundaries, we use the assumptions analogous to Eqs. (I-13a) and (I-14a) for the pressure gradients.

F. Putting It All Together for the Momentum Equation.

Owing mainly to complexities of notation, it seems unwise to try to write down the equations for the viscous code. It appears more logical to outline the steps, which are highly repetitive, and let it go at that.

We have not made a detailed study of the time centering of the viscous acceleration, but have made it fit our code as it stands. Given the coordinates at n and velocities at $n-\frac{1}{2}$, the first step is to calculate the σ 's by using Eqs. (II-7), (II-8) and (II-2). The second step is to calculate the $\vec{F}_{t+\frac{1}{2}}$ for each subzone by adding together the contributions from Eq. (II-6a) for all sides and the faces of the triangles for that subzone. Then, as with the pressure, we get a viscous acceleration by using Eq. (I-11).

G. The Energy Equation.

The viscosity makes a contribution to the energy equation which corresponds to the effects in the momentum equation. For each viscous triangle,

this energy change per unit volume is given by¹³

$$S = \sigma_{ik} \frac{\partial v_i}{\partial x_k} = \sigma_{rr} \dot{r}_r + \sigma_{rz} \dot{r}_z + \sigma_{\theta\theta} \frac{\dot{r}}{r} + \sigma_{zr} \dot{r}_r + \sigma_{zz} \dot{z}_z \quad (\text{II-9})$$

For each zone, these energy changes are summed to find the energy change for the whole zone due to the viscous effects. The fact that the energy change is applied to the whole zone is an important point, and the section on the TTS will reconsider this procedure.

H. Conclusion.

The viscosity method described above has helped prevent mesh tangling for a number of problems in JANUS. The coefficients, μ and λ , must be chosen large enough to prevent tangling, yet not so large as to change the physics of the problem. Reasoning and experience have shown that the coefficients should be proportional to the density, ρ . Experience has indicated that perhaps the coefficients should depend on the mesh spacing. However, we were never able to make the viscosity a general panacea for prevention of mesh tangling. It acts as a velocity-smoothing device, whereas sometimes one needs a coordinate-smoothing code. This need led to the development of rezoning.²

The action of the viscosity code can be illustrated by a simple example. Suppose one has a mesh, which, owing to some perturbation, develops a velocity pattern as shown in Fig. 7. Because the calculation is essentially a momentum transfer, any large velocities of alternating direction are partly transferred to adjacent points, and the oscillations are reduced on the next cycle.

III. A TWO-DIMENSIONAL ARTIFICIAL VISCOSITY

A. One-Dimensional Artificial Viscosities.

In the one-dimensional plane case, the Richtmyer-von Neumann artificial viscosity^{14,15} for approximating shocks can be written in two equivalent forms

$$q = b^2 \rho (\Delta x)^2 \rho_0^2 \left(\frac{\partial u}{\partial t} \right)^2 \quad \text{if } \frac{dl}{dt} < 0, \quad (\text{III-1a})$$

and

$$q = b^2 \rho (\Delta x)^2 \left(\frac{\partial v}{\partial x} \right)^2 \quad \text{if } \frac{\partial v}{\partial x} < 0. \quad (\text{III-1b})$$

In this case, the two forms are equivalent because the changes in volume, U , are directly related to

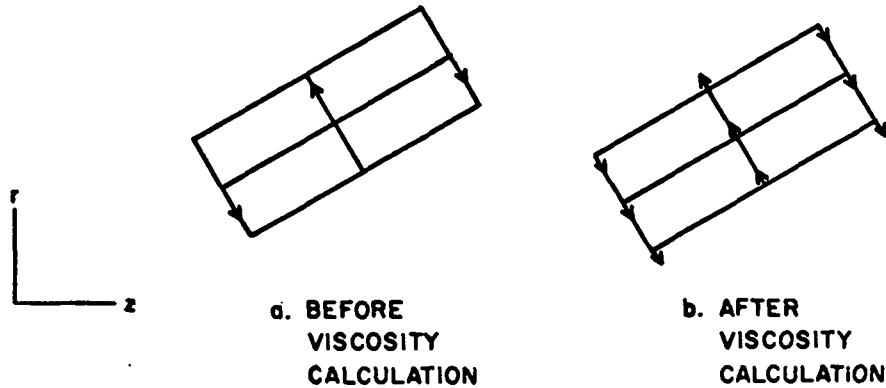


Fig. 7. Velocity smoothing with a viscosity calculation.

the velocity gradients by the equation of continuity,

$$\rho_0 \frac{\partial v}{\partial t} = \frac{\partial v}{\partial x} \quad (\text{III-2})$$

In Eq. (III-1), Δx is the original zone spacing. By including it in the coefficient, one is essentially adjusting the size of q so that the shock will be spread over a desired number of zones. One could also write Eq. (III-1b) in the form

$$q = b^2 \rho (\Delta x)^2 \left(\frac{\partial v}{\partial x} \right)^2, \quad (\text{III-3})$$

where (Δx) is the spacing at the time q is calculated.

B. The Difficulties with Artificial Viscosities in Two Dimensions.

In two dimensions, for a quadratic mesh in which there are essentially two "directions" in which the zone may be squeezed; i.e., a shock may come in from either of or a combination of two directions, it is not so easy to decide what $(\Delta x)^2$ or $(\Delta y)^2$ should be, and in the case of Eq. (III-3), it is not clear what to use for $\partial v / \partial x$. MAGEE,¹⁰ adopted the form of Eq. (III-1a) with the assumption that $(\Delta x)^2$ could be replaced by the original area of the zone, which is, in a way, a measure of the spacing. This has worked well in MAGEE because in that code the aspect ratios are always kept relatively small. We have used this same form in JANUS, but for large aspect ratios (which give large areas), the shock term becomes very large, spreads the shock over too many zones, and also forces the problem to run at very fine time intervals.

However, this is not the only difficulty. Even worse is the fact that, for large aspect ratios, a

small motion approximately perpendicular to the length of the zone (Fig. 8) can produce large volume changes in one cycle. This, in turn, produces large entropy and pressure changes for the whole zones. These inordinately large or small pressures are used in the momentum equation on the next cycle, which tends to make the points at the other end of the zone move upward, long before any real physical signal should reach them. This leads to oscillations in the mesh. We have traced this effect in a number of problems, and Schulz¹⁶ has called attention to it.



Fig. 8. Large volume changes due to small motion.

Schulz devised a very neat method of dealing with this difficulty. He, essentially, defines two directions, \vec{R}_l and $-\vec{R}_k$, associated with each zone (corresponding roughly to the length and width of the zone). He then derives a separate q term for each of the four sides of the zone, by taking the projections of the appropriate velocity differences along the appropriate direction. Thus, for a long, thin zone, different q terms are obtained at each end of the zone, and are used in calculating the momentum equation for the points at their respective ends of the zone. This seems highly desirable.

C. Use of the Viscous Code as the Basis for a Two-Dimensional q Term.

When faced with the necessity for deriving a two-dimensional artificial viscosity, especially one for zones with large aspect ratios, which to us

means getting a q term at each end of the zone as Schulz did, it occurred to us that our viscosity code essentially separates the ends of the zone by the use of the viscous triangles (Fig. 6). It would be appropriate to try to develop a two-dimensional q term for each triangle and include it in the viscous-stress tensor. Then the viscous code could be a framework for using the σ 's properly in the momentum and energy equations.

D. Selecting Two Directions.

For a two-dimensional q term in a triangle, two directions are needed, because the triangle might be squeezed from one direction and expanding in another. We have tried several methods, including Schulz's, for the whole zone, but have found that for peculiarly shaped zones, our method requires judicious selection of directions for each triangle. The method we used defines the directions in two ways, and then weights the two choices depending on the "length" and "width" of the triangle.

Consider any viscous triangle as shown in Fig. 9, where O2 is the side of the zone, with the midpoint at 1. Define one set of directions related to the "altitude,"

$$\vec{R}_a^1 = \text{unit vector along } 18 = r_a \vec{i} + z_a \vec{k}, \quad (\text{III-4})$$

$$\text{where } r_a = (r_8 - r_1) / \ell_{18}, \quad z_a = (z_8 - z_1) / \ell_{18}, \quad \ell_{18} = [(r_8 - r_1)^2 + (z_8 - z_1)^2]^{\frac{1}{2}},$$

and

$$\vec{R}_a^1 = \text{unit vector perpendicular to } \vec{R}_a^1 \text{ (rotated clockwise)} = -z_a \vec{i} + r_a \vec{k}. \quad (\text{III-4a})$$

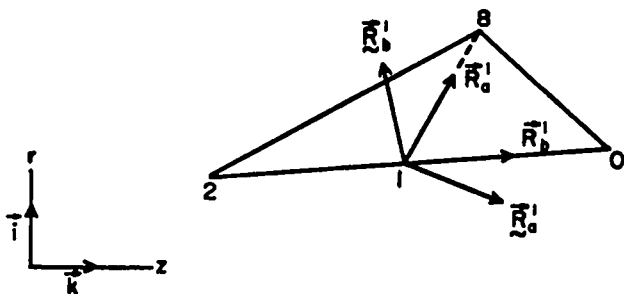


Fig. 9. Specifying directions for a viscous triangle.

Define a second set of directions related to the "base" of the triangle,

$$\vec{R}_b^1 = \text{unit vector along line } 10 = r_b \vec{i} + z_b \vec{k} \quad (\text{III-5})$$

$$\text{where } r_b = (r_0 - r_1) / \ell_{01}, \quad z_b = (z_0 - z_1) / \ell_{01}, \quad \ell_{01} = [(r_0 - r_1)^2 + (z_0 - z_1)^2]^{\frac{1}{2}},$$

and

$$\vec{R}_b^1 = \text{unit vector perpendicular to } \vec{R}_b^1 \text{ (rotated counterclockwise)} = z_b \vec{i} - r_b \vec{k}. \quad (\text{III-5a})$$

We now average these unit vectors, weighted by lengths.

$$\vec{R}_a = (\ell_{18} \vec{R}_a^1 + \ell_{01} \vec{R}_b^1) / (\ell_{18} + \ell_{01}), \quad (\text{III-6})$$

$$\vec{R}_b = (\ell_{18} \vec{R}_a^1 + \ell_{01} \vec{R}_b^1) / (\ell_{18} + \ell_{01}).$$

Thus, the directions emphasized are those related to the long, thin aspect of the triangle. They are also perpendicular unit vectors.

E. The q Term for a Viscous Triangle.

If one wishes to take into account shocks from either of two, or a combination of both, directions, it seems apparent that the velocity gradient form, Eq. (III-1b), of the one-dimensional Richtmyer-von Neumann artificial viscosity should be used as a basis. As we have said before, the volume form, Eq. (III-1a), makes no distinction about direction.

What we have done, then, is to add two terms of the form of Eq. (III-1b), one for each of the directions a and b defined in the previous section. We represent this as

$$\tau_{q_{1i}} = -b^2 \rho \left[(\Delta L)_a^2 \left(\frac{\Delta v}{\Delta L} \right)_a^2 + (\Delta L)_b^2 \left(\frac{\Delta v}{\Delta L} \right)_b^2 \right]. \quad (\text{III-7})$$

The negative sign arises because we are transferring q from the second (pressure) term to the third term in Eq. (II-3).

To calculate Eq. (III-7), consider a viscous triangle (Fig. 10). We know the velocities at

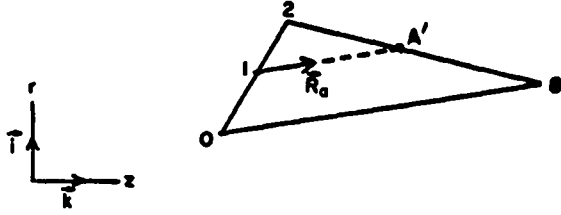


Fig. 10. Finding A' in a viscous triangle.

points 0, 2, and 8 and assume that each velocity component is defined by a plane function over the triangle, as described in Sec. II. Then for each of the directions \vec{R}_a and \vec{R}_b , a corresponding $(\Delta v/\Delta L)_a$ or $(\Delta v/\Delta L)_b$ is found for the triangle as follows. Consider \vec{R}_a .

Using the direction \vec{R}_a , one finds where a line drawn from point 1 intersects one of the other sides of the triangle. Suppose it is at A' . The coordinates will be given by

$$r_{A'} = \frac{r_a(r_8 z_2 - r_2 z_8) + (r_8 - r_2)(r_1 z_a - z_1 r_a)}{r_a(z_2 - z_8) + z_a(r_8 - r_2)}, \quad (III-8)$$

and

$$z_{A'} = \frac{(z_8 - z_2)(r_1 z_a - z_1 r_a) + z_a(r_8 z_2 - r_2 z_8)}{r_a(z_2 - z_8) + z_a(r_8 - r_2)}.$$

The velocities at points 1 and A' are now known.

$$\begin{aligned} \vec{v}_1 &= \dot{r}_1 \vec{i} + \dot{z}_1 \vec{k}, \quad \dot{r}_1 = \frac{\dot{r}_0 + \dot{r}_2}{2}, \quad \dot{z}_1 = \frac{\dot{z}_0 + \dot{z}_2}{2}, \\ \vec{v}_{A'} &= \dot{r}_{A'} \vec{i} + \dot{z}_{A'} \vec{k}, \quad \dot{r}_{A'} = \dot{r}_2 + \dot{r}_r(r_{A'} - r_2) \\ &+ \dot{r}_z(z_{A'} - z_2), \quad \dot{z}_{A'} = \dot{z}_2 + \dot{z}_r(r_{A'} - r_2) \\ &+ \dot{z}_z(z_{A'} - z_B). \end{aligned} \quad (III-9)$$

The next step is to find the relative velocities along direction \vec{R}_a ; i.e.,

$$(\Delta v)_a = \vec{R}_a \cdot (\vec{v}_{A'} - \vec{v}_1) = r_a(\dot{r}_{A'} - \dot{r}_1) + z_a(\dot{z}_{A'} - \dot{z}_1). \quad (III-10)$$

Because we want a q term only in case of squeezing, we set

$$(\Delta v)_a = 0 \quad \text{if } (\Delta v)_a > 0. \quad (III-10a)$$

From Eq. (III-8) one can get

$$|\vec{r}_{1A'}| = [(r_{A'} - r_1)^2 + (z_{A'} - z_1)^2]^{1/2}, \quad (III-11)$$

and, hence,

$$\left(\frac{\Delta v}{\Delta L}\right)_a = (\Delta v)_a / |\vec{r}_{1A'}|. \quad (III-12)$$

A shorter way of calculating this same result, which eliminates some of the required testing (not mentioned above) can be derived from Eqs. (III-9) and (III-10).

$$\begin{aligned} \left(\frac{\Delta v}{\Delta L}\right)_a &= \frac{(\dot{r}_{A'} - \dot{r}_1) \cdot \vec{R}_a}{|\vec{r}_{1A'}|} = \frac{\{i[(\dot{v}_r) \cdot \vec{r}_{1A'}] + k[(\dot{v}_z) \cdot \vec{r}_{1A'}]\} \cdot \vec{R}_a}{|\vec{r}_{1A'}|} \\ &= \{i[(\dot{v}_r) \cdot \vec{R}_a] + k[(\dot{v}_z) \cdot \vec{R}_a]\} \cdot \vec{R}_a \\ \left(\frac{\Delta v}{\Delta L}\right)_a &= \dot{r}_r r_a^2 + (\dot{r}_z + \dot{z}_r) r_a z_a + \dot{z}_z z_a^2. \end{aligned} \quad (III-13)$$

This also is set equal to zero if it is positive (indicating expansion). This form is interesting, as it shows the value of $(\Delta v/\Delta L)_a$ to be independent of the choice of points 1 and A' . This is logical because the velocities have been assumed to be plane functions over the triangle. For $(\Delta v/\Delta L)_b$, there would be a similar expression involving r_b and z_b .

To find the values of $(\Delta L)_a^2$ and $(\Delta L)_b^2$ needed, we used the average dimension of the zone in that direction (Fig. 11). Namely,

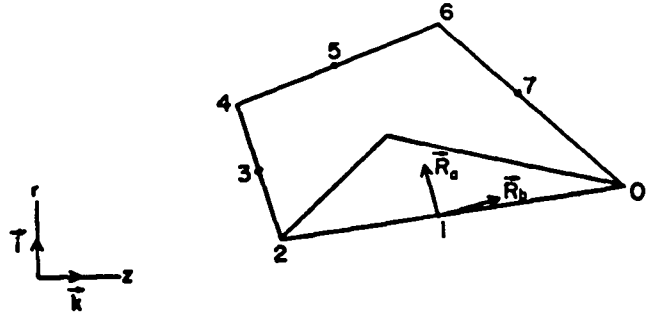


Fig. 11. Finding $(\Delta L)_a^2$ and $(\Delta L)_b^2$.

$$(\Delta L)_a^2 = \{\vec{R}_a \cdot \vec{R}_{15}\}^2 = \{r_a(r_5 - r_1) + z_a(z_5 - z_1)\}^2,$$

$$(\Delta L)_b^2 = \{\vec{R}_b \cdot \vec{R}_{37}\}^2 = \{r_b(r_7 - r_3) + z_b(z_7 - z_3)\}^2.$$

$$(III-14)$$

It is found unwise to use dimensions from the triangle here, because, in some cases, these dimensions become small (points squeezing together) just when one wants the q term to remain large.

F. Incorporation of the q Term into the Viscous-Stress Tensor.

The previous section shows how to evaluate Eq. (III-7) for a viscous triangle, except for the factor ρ . At first, we used the ρ of that zone, but later we found that using the actual density of the viscous triangle helped problems run much further without tangling. This necessitates calculating these triangular masses at the start of the problem, and carrying them in storage, which requires more storage. However, we were concentrating on finding something to prevent mesh tangling, rather than on code efficiency. Code efficiency can be achieved later if one finds a good method.

Having evaluated $\tau_{q_{ii}}$ for each viscous triangle, we then added this term to the diagonal terms of the viscous-stress tensor

$$\sigma_{ij} = \mu \left(\frac{\partial v_i}{\partial x_j} + \frac{\partial v_j}{\partial x_i} \right) + \delta_{ij} (\nabla \cdot \vec{v}) + \delta_{ij} \tau_{q_{ii}}, \quad (\text{III-15})$$

and removed the one-dimensional q term from the pressure. In this way, we could use our regular viscous code to try out the two-dimensional artificial viscosity. Analysis of a simple plane problem showed that the same q_{ii} had to be used in each of the diagonal terms, to preserve uniform motion.

G. Conclusions and Results.

The method presented here has been tested in some plane, cylindrical, and spherical problems with $\lambda = \mu = 0$ and $b^2 = 1.44$. All retained their symmetry, and agreed closely with corresponding problems in which a true one-dimensional q term [$q = b^2 \rho (\Delta R/V)^2 (\Delta V/\Delta t)^2$] was used. This method was also used in several slightly nonspherical problems with long thin zones which developed mesh tangling with the volume form, Eq. (III-1a) of the q term, and it enabled these problems to run much further than before. However, at later times, even with the two-dimensional q term, these problems developed difficulties. We tried a number of devices to eliminate these difficulties, such as using small values for λ , μ along with the τ term, adding a linear term to the quadratic term as suggested by Meyer,¹⁷ and us-

ing smaller time intervals. None of these devices appeared to do a great deal of good, but the trials were limited. Study of movies of some of these problems showed that the tangling was not a one-dimensional type of oscillation, but more the type of situation described in Fig. 8. This led us to look for further means of isolating the ends of long, thin zones from each other, and the energy equation seemed to be the place to look.

IV. TTS (TEMPORARY TRIANGULAR SUBZONING)

A. Isolating the Ends of a Zone for Energy Calculations.

In Sec. III, we described a method for isolating the ends of long, thin zones from each other as far as the artificial viscosities are concerned. However, the separate internal energies calculated for each viscous triangle are all lumped together and dispersed through the whole zone. It appears to us that Schulz¹⁶ also does this in his method.

Because the artificial viscosities are applied to the points at one end of a zone, it seems a logical next step to confine the energy change arising from these q terms, temporarily, to the end of the zone where they are produced. Using different energies in different viscous triangles, one can then get different pressures for the triangles of the zone. These could then be used in the momentum equation, along with the different q terms.

B. Putting the TTS into JANUS.

The sequence of calculations for one cycle of JANUS can be represented as follows.

$$\left[a^{n-1}, v^{n-\frac{1}{2}} \right] \left[R^n \right] \left[a_V^n, \Delta E_V^{n-\frac{1}{2}} \right] \left[\tau^n, P^n, E^n \right]. \quad (\text{IV-1})$$

Each bracket represents a pass through the mesh. On the first pass, the accelerations at times $n-1$ and a^{n-1} are calculated from the coordinates, R^{n-1} , and pressures, P^{n-1} , both known from the last cycle. Immediately, the velocities at $n-\frac{1}{2}$ are calculated, using $v^{n-\frac{1}{2}}$ and R^{n-1} . The viscous calculations are made on the third pass. From the σ 's, one can get the viscous accelerations, a_V^n , which are saved to add in with the acceleration from the pressures on the first pass of the next cycle. The change in internal energy due to viscosity, $\Delta E_V^{n-\frac{1}{2}}$, can also be calculated from the σ 's. On the fourth pass, the new volumes, τ^n , are evaluated. Also the $\Delta E_V^{n-\frac{1}{2}}$

are added to the E^{n-1} to give an \tilde{E}^{n-1} . Then the conservation of internal energy,

$$E^n = \tilde{E}^{n-1} - \frac{1}{2}(P^n + P^{n-1})(\tau^n - \tau^{n-1}), \quad (IV-2)$$

and the equation of state,

$$P^n = P(\tau^n, E^n), \quad (IV-3)$$

are solved together, simultaneously or by iteration, to get P^n , E^n , and τ^n .

Using the TTS method, the calculation is similar.

$$\left(\underline{v}^{n-\frac{1}{2}}, R^n \right) \left(\underbrace{\Delta E_V^{n-\frac{1}{2}}}_{\Delta} ; \underbrace{\tau^n, P^n, E^n}_{\Delta} ; \underbrace{\tau^n, P^n, E^n, T^n}_{\text{zone}} ; a_{V+P}^n \right).$$

We omit the calculation of a^{n-1} in the first pass and combine the velocity and coordinate calculations into a single pass. As will be explained, a^{n-1} has already been calculated on the last pass of the previous cycle. In the third pass, the σ 's and the $\Delta E_V^{n-\frac{1}{2}}$ from them are evaluated. At the same time, for each triangle, a new τ^n is calculated (an old τ^{n-1} is also calculated by deadvancing the coordinates from n to $n-1$). The $\Delta E_V^{n-\frac{1}{2}}$ is added to E^{n-1} to give \tilde{E}^{n-1} as before. The old E^{n-1} and P^{n-1} are for the whole zone (the same for all triangles), as these are the only quantities saved. Then for each triangle, we use Eqs. (IV-2) and (IV-3) to get new E^n and P^n .

At this point, for each triangle, the P^n are added to the viscosity-stress tensor, as is often done in the literature (Ref. 13, Ch. II).

$$\sigma_{ij} = \mu \frac{\partial v_i}{\partial x_j} + \frac{\partial v_j}{\partial x_i} + \delta_{ij} (\lambda \nabla \cdot \vec{v} + \tau_{ij} q_{ij} - P^n). \quad (IV-4)$$

Now if we use the IGA-MACO method for integrating the tensor, as described in Sec. II, we are at the same time using an IGA-MACO method for evaluating $-\int \rho d\vec{S}$, as described in Sec. I, except that we are using different pressures in different viscous triangles of the same zone. This is what we want to do.

This integration leads to an acceleration, which we shall call

$$a_{V+P}^n = \text{acceleration due to viscosity and pressure.}$$

(IV-5)

This quantity is stored for use on the first pass of the next cycle.

After using the triangular pressures to get a_{V+P}^n , we sum the energies of the viscous triangles of each zone, and, from Eqs. (IV-2) and (IV-3), calculate new τ^n , P^n , E^n , and T^n for the whole zone. This amounts to smearing out the energies of the triangles over the zone. These values are then used as P^{n-1} and E^{n-1} on the next cycle.

C. General Observations.

Quadrilateral meshes with large aspect ratios are notorious for tangling or developing ripples unless auxiliary devices, such as rezoning, are used. Many of these motions are not physically real. On the other hand, triangular meshes tend to prevent tangling, because as points try to cross over opposite sides, the volumes quickly become small and the pressures grow very large, tending to oppose the undesirable motion. However, triangular meshes tend to be stiff. The method described above is an attempt at a compromise, to use the good feature of a triangular calculation to help solve the weakness in a quadrilateral mesh. We hope that because the triangular calculation is used only temporarily for the acceleration calculation, after which the energy is redistributed over the whole zone, the tendency to stiffness will be diminished.

We have used this method in JANUS on some of the problems that had experienced difficulties, and they ran without oscillations or tangling until very late times. These problems are described in Sec. V. Time has not allowed a detailed study of the separated or individual effects of the gradients, the viscosity calculation, the two-dimensional artificial viscosity, and the temporary triangular subzoning in these problems, but using all of them together greatly reduced the mesh tangling. There may be some stiffening, due probably to the TTS, but we have not had time to investigate this thoroughly. Also, aside from the usual plane, cylindrical, and spherical problems, it is difficult to find problems to really test two-dimensional hydrodynamic calculations.

Our main purpose has been to present some promising ideas we have tried, some of which appear to have been overlooked by workers in this field. Some of the descriptions are brief and vague, because the equations and notations are cumbersome and

complicated, and we feel that presenting the basic ideas is more important.

V. EXAMPLES

The figures in this section show an example problem with zones of large aspect ratios. The figures show only those parts of the mesh which illustrate the results. The problem is "almost" planar, being slightly thinner at the top than at the bottom. It is subjected to two "almost" planar shock waves passing from left to right.

Figures 12 through 15 show the behavior of this system when a one-dimensional q term of the bulk type, Eq. (III-1), namely

$$q = 1.44 \rho (\Delta z)^2 \rho_0^2 \left(\frac{\Delta U}{\Delta t} \right)^2, \quad (V-1)$$

was used. This q was added to the pressure in both the momentum and energy equations as described in Ref. 1. We used the integrated gradients (IGA-MACO) of Sec. I, but none of the other devices described in the later sections of this report. Note the twisting of the mesh at the later times (Figs. 14 and 15).

Figures 16 through 19 show the behavior of exactly the same problem at exactly the same times, but using the rest of the methods described in this report, an approach we have dubbed the 1CVAEA (One Cycle Viscous Triangle Energy, Acceleration) Method. Note that the mesh is considerably less twisted at the corresponding times.

These two methods have also been compared in similar problems for perfect planes, cylinders, etc. The plane problems agreed at late times to within 0.33%, and the cylindrical problems agreed within about 1.5%. The problems run using the one-dimensional q term lagged the problem run using the 1CVAEA calculations. This could indicate that the latter method imparts some stiffness to the mesh. However, we were pleased that the method retains symmetry in symmetrical problems.

We have run some other test problems, but much further work and analysis of problems and methods needs to be done. However, we think the results thus far are encouraging.

ACKNOWLEDGMENTS

Because this work has been pursued, off and on, over a period of years, it is impossible to list by

name all those who have contributed in one way or another. Hence, without listing names, we wish to thank those who have allowed us to take time to pursue these investigations, those who have taken time to discuss the ideas and results with us, and those who may have contributed in any other ways.

REFERENCES

1. Philip L. Browne and Martha S. Hoyt, "HASTI: A Numerical Calculation of Two-Dimensional Lagrangian Hydrodynamics Utilizing the Concept of Space Development Time Steps," Los Alamos Scientific Laboratory Report LA-3324-MS (September 1965).
2. Philip L. Browne, "Rezone: A Proposal for Accomplishing Rezoning in Two-Dimensional Lagrangian Hydrodynamics Problems," Los Alamos Scientific Laboratory Report LA-3455-MS (March 1966). (A more up-to-date discussion with some results was published in The Proceedings of the 1968 IFIP Congress, Edinburgh, Scotland, Supplement, p. I 131.)
3. Philip L. Browne and Karl B. Wallick, unpublished report, 1964-66.
4. W. F. Noh, "CEL: A Time-Dependent, Two-Space Dimension, Coupled Eulerian Lagrange Code," Lawrence Radiation Laboratory, Livermore, Report UCRL 7463 (August 1963).
5. Mark L. Wilkins, "Calculation of Elastic-Plastic Flow," Lawrence Radiation Laboratory, Livermore, Report UCRL 7322 (April 1963).
6. Philip L. Browne and Karl B. Wallick, LASL, unpublished report, 1964.
7. Philip L. Browne and Karl B. Wallick, LASL, unpublished report, 1970.
8. Francis H. Harlow and Anthony A. Amsden, "Fluid Dynamics - an Introductory Text," Los Alamos Scientific Laboratory Report LA-4100 (May 1970), p. 77.
9. Philip L. Browne and Leland R. Stein, LASL, unpublished work, 1966.
10. S. R. Orr, LASL, unpublished work, 1959.
11. Walter Goad, "WAT: A Numerical Method for Two-Dimensional Unsteady Flow," Los Alamos Scientific Laboratory Report LAMS-2365 (November 1960).
12. R. Aris, Vectors, Tensors and the Basic Equations of Fluid Mechanics, Prentice Hall, Inc. Englewood Cliffs, N. J., 1962, Ch. 8.
13. L. D. Landau and E. M. Lifschitz, Fluid Mechanics, Pergamon Press, New York, 1959, p. 48-9, 232.
14. J. von Neumann and R. D. Richtmyer, J. Appl. Phys. 21, 232 (1950).
15. R. D. Richtmyer, Difference Methods for Initial

Value Problems, Interscience Publishers, Inc.,
New York, 1957, p. 208.

16. William D. Schulz, "Two-Dimensional Lagrangian Hydrodynamics Difference Equations," Lawrence Radiation Laboratory, Livermore, Report UCRL 6776 (April 1963).
17. Kenneth A. Meyer, "Artificial Viscosities Considered for Use in the CIRCE Lagrangian Hydrocode," Los Alamos Scientific Laboratory Report LA-4383-MS (CONF-RD)(April 1970).

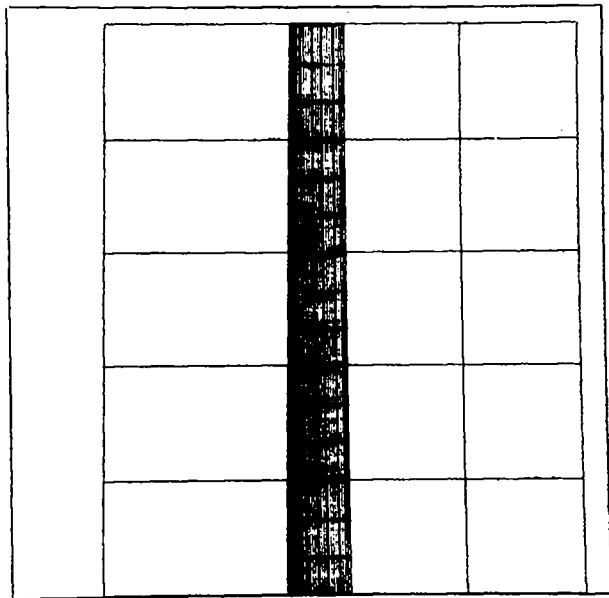


Fig. 12. Initial configuration, $t=0.000000$.

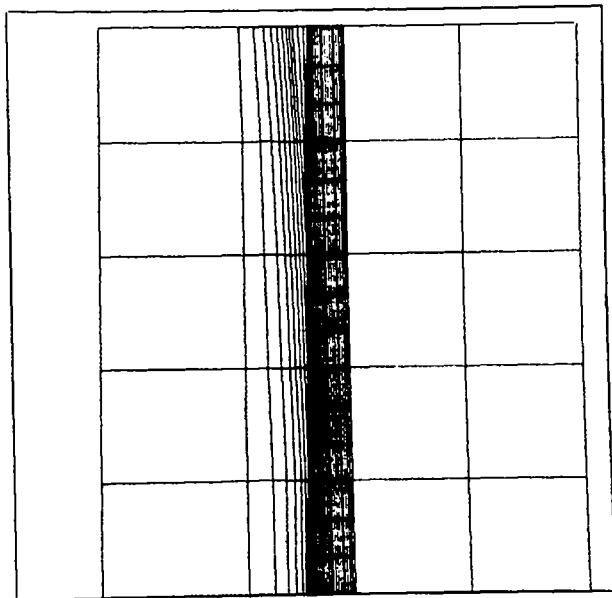


Fig. 13. Configuration at an early time, $t=0.0450000$, as first shock is passing through.

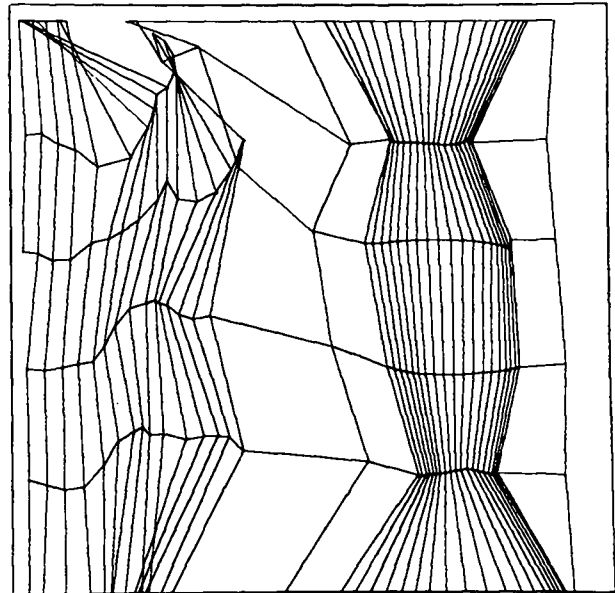


Fig. 14. Configuration at later time, $t=0.5000000$, after first shock has passed by. Note the distortions of the mesh.

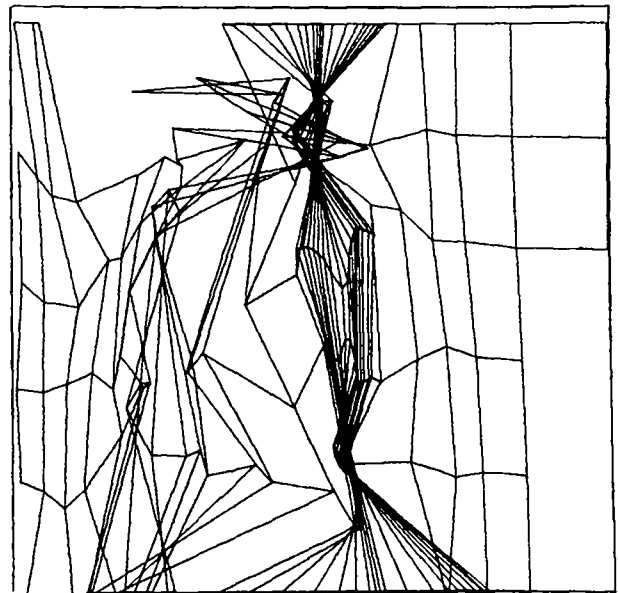


Fig. 15. Very late time, $t=1.0000000$, in problem when mesh is badly twisted.

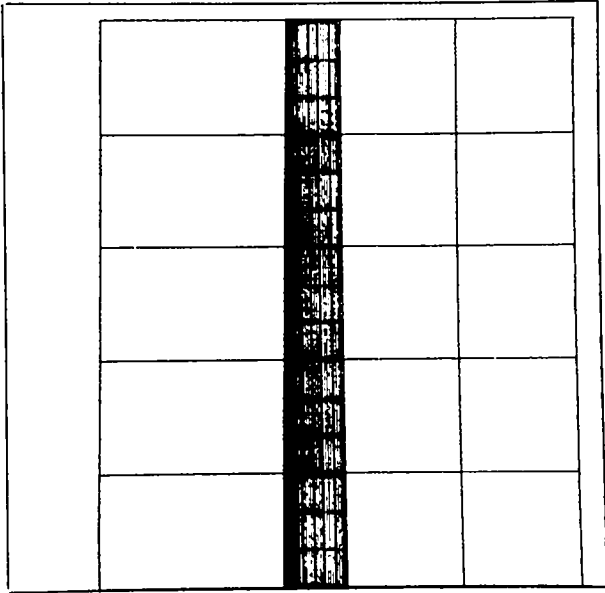


Fig. 16. Initial configuration, $t=0.000000$.

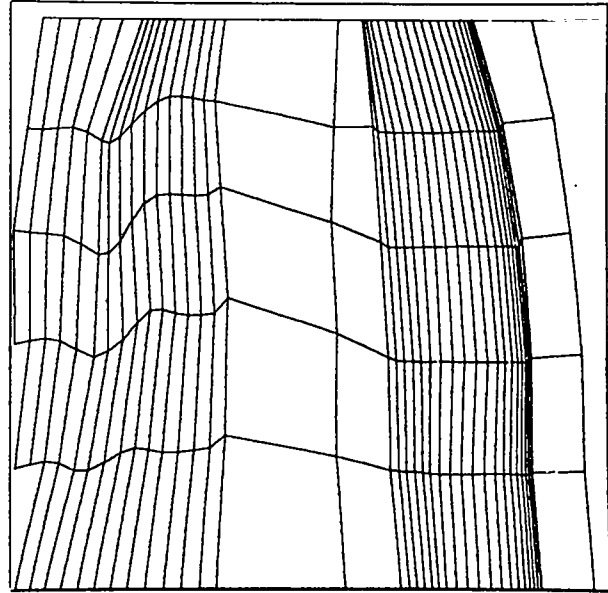


Fig. 18. Configuration at later time (same time as Fig. 14).

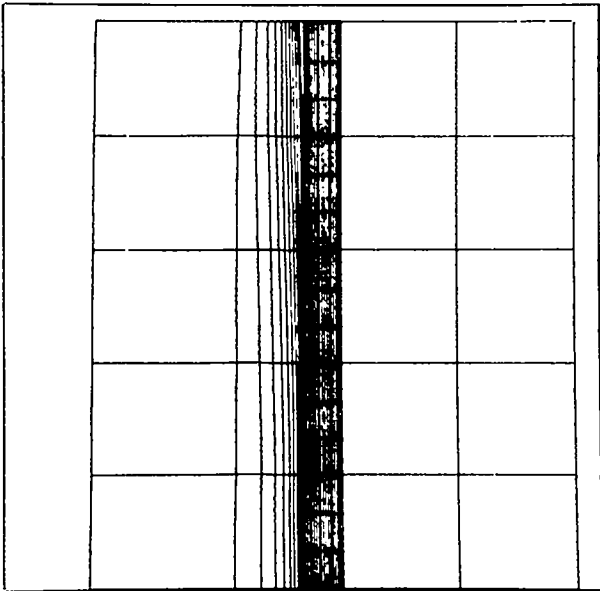


Fig. 17. Configuration at an early time, $t=0.045000$.

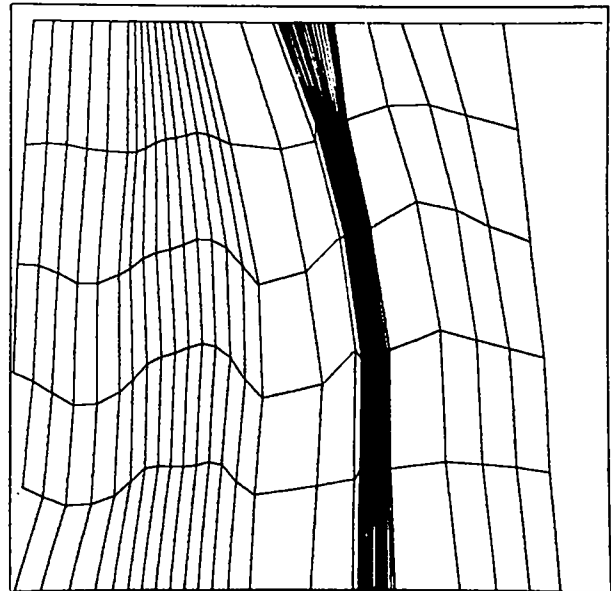


Fig. 19. Configuration at very late time (same time as Fig. 15).